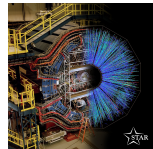


Longitudinal Double-spin Asymmetry for Inclusive Jet and Dijet Production in pp Collisions at $\sqrt{s} = 510$ GeV

Zilong Chang

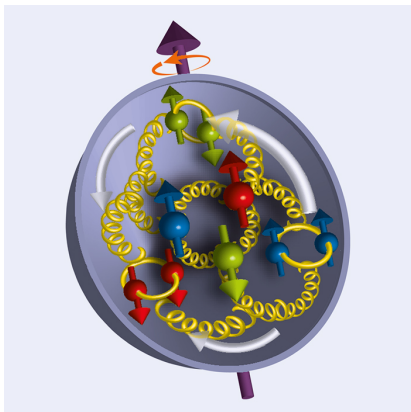
Brookhaven National Laboratory, Upton, New York 11973

September 10th, 2019



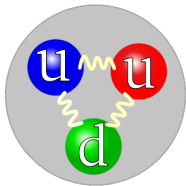
- **Introduction**
 - Parton distribution function
 - Gluon polarization in the proton
- **Longitudinal double-spin asymmetry for inclusive jet and dijet production in pp collisions at $\sqrt{s} = 510$ GeV**
 - Jet reconstruction
 - Underlying events contribution to jet p_T and A_{LL}
 - Inclusive jet and dijet A_{LL} results
- **Other inclusive jet and dijet A_{LL} measurements and STAR forward upgrade**
- **Conclusion**

Introduction



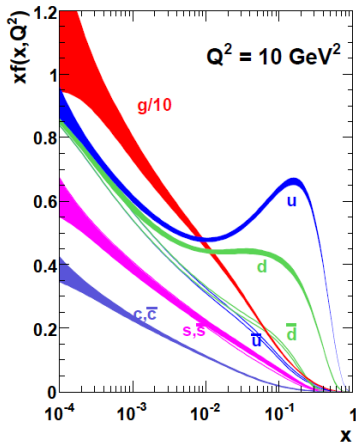
The Proton Structure

- **Constituents:** quarks and gluons



- **Parton distribution functions:** $f(x, Q^2)$, the probability of a probe at momentum transfer Q^2 encountering a parton in the proton with momentum fraction x
- gluons dominate at low x

- $xf(x, Q^2 = 10 \text{ GeV}^2)$ vs. x for quarks and gluons, MSTW, EPJC63, 189



What about proton spin?

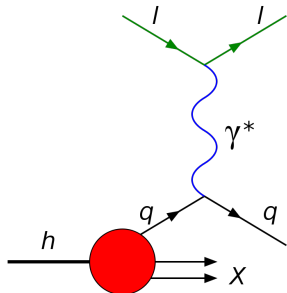
The Proton Spin

Proton spin sum rule:

$$S_z = \frac{1}{2} = \frac{1}{2}\Delta\Sigma + \Delta G + L_{q,g}$$

Deep inelastic scattering:

- Quark contribution $\Delta\Sigma$: constrained
 $\Delta\Sigma = 0.254 \pm 0.042$, Leader et al, PRD 82, 114018
- Gluon contributions ΔG : **poorly** constrained
Fixed targets experiments \rightarrow Limited in $x - Q^2$ space
Constrained through scaling violation
- $L_{q,g}$: not constrained

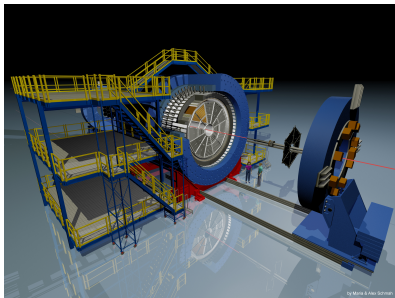
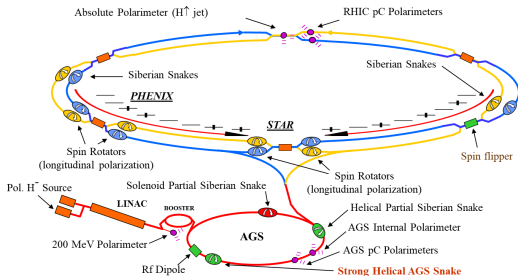


Hadron-hadron scattering:

Asymptotic freedom at short distances \rightarrow parton-parton scattering

Direct access of gluons

RHIC and STAR Detectors



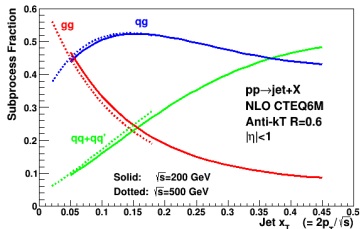
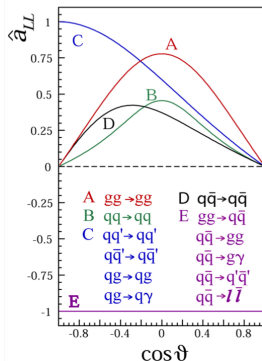
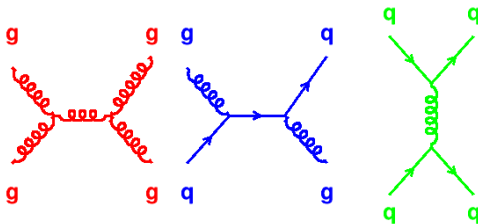
- One and only polarized hadron collider
- Beam polarization measurements: H-jet and pC polarimeter
- STAR detector: 2π in azimuthal ϕ , and η up to 3.9

- Tracking with TPC: $|\eta| < 1.3$
- EM energy and triggering with:
BEMC: $-1.0 < \eta < 1.0$,
EEMC: $1.0 < \eta < 2.0$
- Relative luminosity monitoring detectors:
VPD, BBC and ZDC

Exploring Gluon Polarization at RHIC

- Define longitudinal double-spin asymmetry A_{LL} for Jets:

$$A_{LL} = \frac{\sigma^{++} - \sigma^{+-}}{\sigma^{++} + \sigma^{+-}} \sim \frac{\Delta f_a \Delta f_b}{f_a f_b} \hat{a}_{LL}$$



- gg and qg dominate jet production + large $\hat{a}_{LL} \rightarrow$ making A_{LL} for jets sensitive to gluon polarization

Mukherjee and Volgelsang, PRD86, 094009

Longitudinal Double-spin Asymmetry A_{LL} for Jets

- Measure number of jets when beams have the same and the opposite helicity, N^{++} and N^{+-}
- Given $P_{B(Y)}$: beam polarizations, and $R = \frac{L^{++}+L^{--}}{L^{+-}+L^{-+}}$: relative luminosity

$$A_{LL} = \frac{1}{P_B P_Y} \frac{N_{++} - R N_{+-}}{N_{++} + R N_{+-}}$$

- Maximum likelihood estimator from data collected during multiple short periods, runs:

$$A_{LL} = \frac{\sum_{run} P_B P_Y (N^{++} - R N^{+-})}{\sum_{run} P_B^2 P_Y^2 (N^{++} + R N^{+-})}$$

Inclusive Jet and Dijet Measurements

STAR has measured a series of inclusive jet

and dijet A_{LL} at $\sqrt{s} = 200$ GeV

- Inclusive jets:

$$x \approx x_T e^{\pm\eta}$$

$$x_T = \frac{2p_T}{\sqrt{s}}$$

- Dijets: two jet correlation unfolds x_1 and x_2 at the leading order

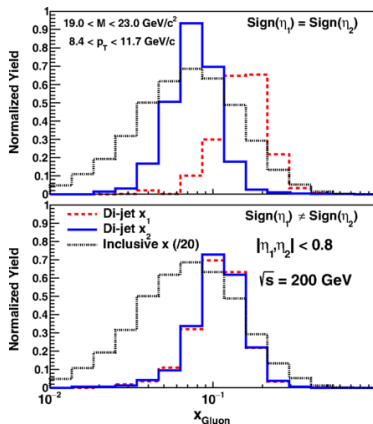
$$x_1 = \frac{1}{\sqrt{s}}(p_{T,3}e^{\eta_3} + p_{T,4}e^{\eta_4})$$

$$x_2 = \frac{1}{\sqrt{s}}(p_{T,3}e^{-\eta_3} + p_{T,4}e^{-\eta_4})$$

$$M = \sqrt{x_1 x_2 s}$$

$$|\cos\theta^*| = \tanh \frac{|\eta_3 - \eta_4|}{2}$$

- x_g as low as ~ 0.05



- Sampled x_g distributions by inclusive jet and dijets at $\sqrt{s} = 200$ GeV

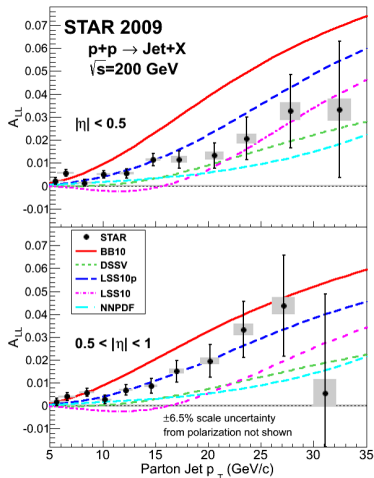
STAR, PRD 95, 071103(R)

Dijet η topology samples different x_1 and x_2 distributions and $\cos\theta^*$ binings, therefore constrains the shape of $\Delta g(x)$ as function of x and \sqrt{s} or η increases, x decreases

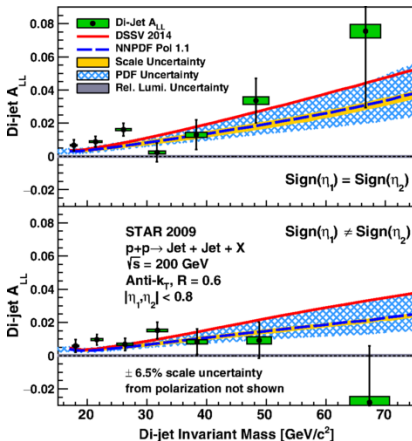
STAR 2009 Inclusive Jet and Dijet A_{LL} Results at $\sqrt{s} = 200$ GeV

- Inclusive jet A_{LL} in two $|\eta|$ bins:
 $|\eta| < 0.5$ and $0.5 < |\eta| < 1.0$, STAR,

PRL115, 092002



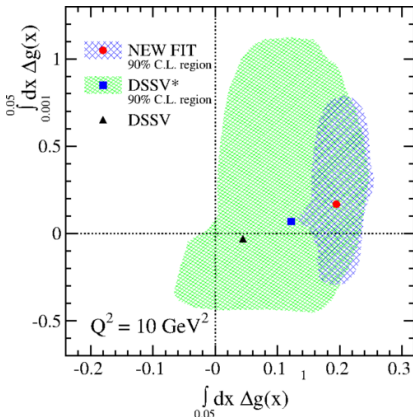
- Dijet A_{LL} in $|\eta| < 0.8$, **barrel region**,
 with two η topologies: $\eta_3\eta_4 > 0$ and
 $\eta_3\eta_4 < 0$ STAR, PRD 95, 071103(R)



Impact of STAR 2009 Inclusive Jet Results

DSSV, PRL113, 012001

- $\int_{0.001}^{0.05} dx \Delta g(x)$ vs. $\int_{0.05}^1 dx \Delta g(x)$
- $\int_{0.05}^1 dx \Delta g(x) = 0.19^{+0.06}_{-0.05}$

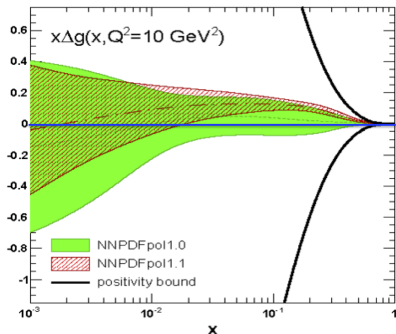


- The vertical uncertainty much larger than the horizontal uncertainty

Even though positive ΔG at $x > 0.05$, to constrain $x\Delta g$ at $x < 0.05$ better:
increasing \sqrt{s} or extending forward in η or both.

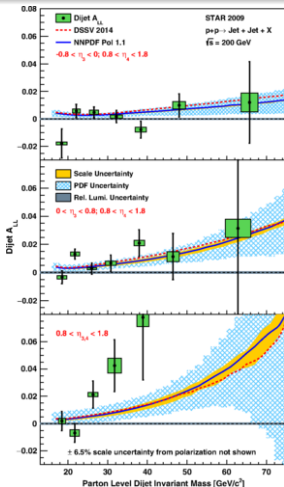
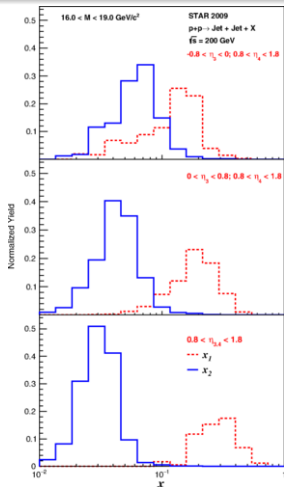
NNPDF, NPB887, 276

- $x\Delta g(x, Q^2)$ vs. x at $Q^2 = 10\text{GeV}^2$
- $\int_{0.05}^{0.5} dx \Delta g(x) = 0.23 \pm 0.07$



- Uncertainty on $x\Delta g$ still large when $x < 0.05$

STAR 2009 Endcap Dijet Results at $\sqrt{s} = 200$ GeV



- Requiring at least one jet in $0.8 < \eta < 1.8$, **endcap region**

- Three η topology bins:

EB-E: $-0.8 < \eta_3 < 0$,
 $0.8 < \eta_4 < 1.8$

WB-E: $0 < \eta_3 < 0.8$,
 $0.8 < \eta_4 < 1.8$

E-E: $0.8 < \eta_{3,4} < 1.8$

- Reach x_g down to 0.01

STAR, PRD 98, 032011

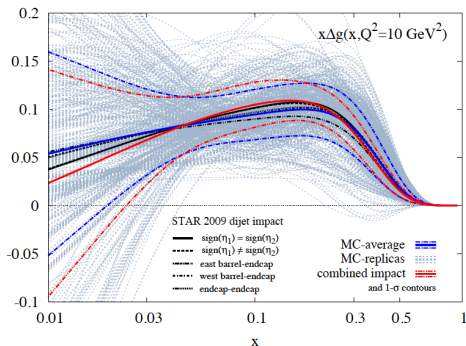
- Sampled x_1 and x_2 distributions for η topologies when

$$16 < M_{inv} < 19 \text{ GeV}/c^2$$

- Dijet A_{LL} for η topologies vs. dijet M_{inv}

Impact of STAR Dijet Results at $\sqrt{s} = 200$ GeV

- $x\Delta g(x, Q^2)$ vs. x , $0.01 < x < 1$ at $Q^2 = 10\text{GeV}^2$
- 2 topologies from dijets within $|\eta| < 0.8$ and 3 topologies from endcap dijets
- Before including STAR dijet results (STAR 2009 inclusive jet results included)
- After including STAR dijet results combined



- The DSSV study shows: $\int_{0.01}^1 \Delta g(x, Q^2 = 10\text{GeV}^2) = 0.296 \pm 0.108$
de Florian et al., arXiv:1902.10548 [hep-ph]

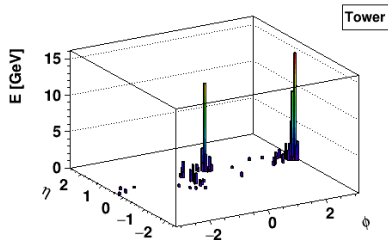
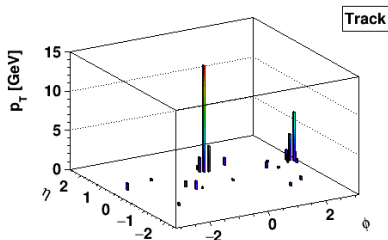
Uncertainty on $x\Delta g$ still large at $x < 0.01$, higher \sqrt{s} ?

**Longitudinal double-spin
asymmetry for inclusive jet and
dijet production in pp collisions
at $\sqrt{s} = 510$ GeV
STAR, Phys. Rev. D 100,
052005**

Differences and improvements from $\sqrt{s} = 200$ GeV

- First measurements at $\sqrt{s} = 510$ GeV
- Optimized trigger to sample low p_T jets according to luminosity increase
- Underlying events correction on jet p_T and its effect on A_{LL}
- Improved Monte Carlo tune to reproduce data better
- Much reduced trigger bias and reconstruction uncertainty
- Finer η topology binning for dijet A_{LL}
- Correlation matrix provided for inclusive jet and dijet A_{LL} results

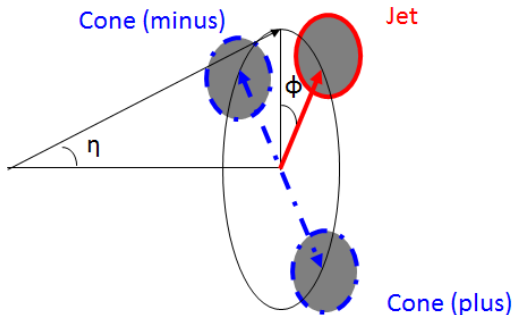
Jet Reconstruction



- Dataset: STAR 2012 longitudinally polarized pp at $\sqrt{s} = 510$ GeV
- Integrated luminosity: 82 pb^{-1}
- Inputs: charged tracks + electro-magnetic towers
- Triggers: B/E-EMC based jet patch triggers, three triggers with different thresholds, 5.4, 7.3 and 14.4 GeV, JP0, JP1 and JP2, optimized to sample low p_T jets that are sensitive to low x_g
- Algorithm: anti- k_T algorithm with $R = 0.5$, helps to reduce soft background and pileup events in the higher \sqrt{s} environment

Underlying Event Correction to Jet Transverse Energy

- Two off-axis cones centered at $\pm \frac{\pi}{2}$ away in ϕ and the same η relative to a given jet are used to estimate underlying event for that jet, ALICE, PRD 91, 112012

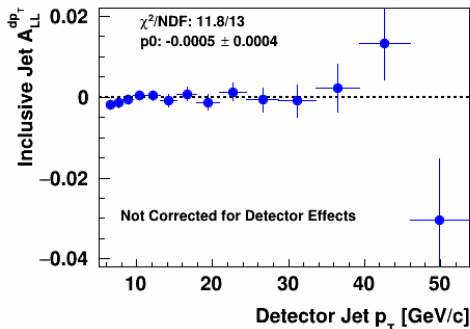


- The underlying event correction on jet transverse momentum:
$$dp_T = \frac{1}{2}(\rho_{plus} + \rho_{minus}) \times A_{jet}, \text{ jet-by-jet}$$
- Scan η dependence of underlying events
- Allow to study the underlying event contribution to jet A_{LL}

Effects of Underlying Events on Measured Jet A_{LL}

- Define underlying event correction dp_T longitudinal double-spin asymmetry:

$$A_{LL}^{dp_T} = \frac{1}{P_A P_B} \frac{\langle dp_T \rangle^{++} - \langle dp_T \rangle^{+-}}{\langle dp_T \rangle^{++} + \langle dp_T \rangle^{+-}}$$



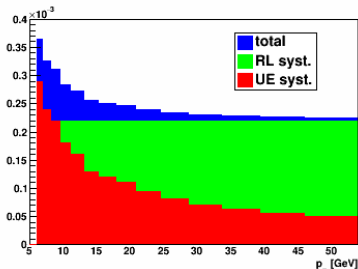
- Underlying event correction dp_T asymmetries are **consistent with zero**

Underlying Event Systematics on Jet A_{LL}

- Given average underlying event correction $\langle dp_T \rangle$ and $A_{LL}^{dp_T}$, potential effect of the underlying event correction, dp_T , on jet A_{LL} :

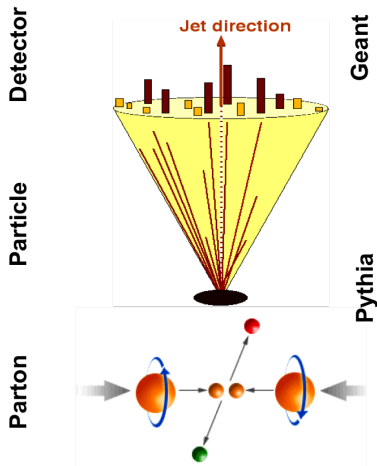
$$\delta A_{LL} = \frac{\int_{p_{T,min} - \langle dp_T \rangle \times A_{LL}^{dp_T}}^{p_{T,max} - \langle dp_T \rangle \times A_{LL}^{dp_T}} \frac{d\sigma}{dp_T} dp_T - \int_{p_{T,min} + \langle dp_T \rangle \times A_{LL}^{dp_T}}^{p_{T,max} + \langle dp_T \rangle \times A_{LL}^{dp_T}} \frac{d\sigma}{dp_T} dp_T}{\int_{p_{T,min} - \langle dp_T \rangle \times A_{LL}^{dp_T}}^{p_{T,max} - \langle dp_T \rangle \times A_{LL}^{dp_T}} \frac{d\sigma}{dp_T} dp_T + \int_{p_{T,min} + \langle dp_T \rangle \times A_{LL}^{dp_T}}^{p_{T,max} + \langle dp_T \rangle \times A_{LL}^{dp_T}} \frac{d\sigma}{dp_T} dp_T}$$

Underlying events shifting the jet cross section differently in the ++ and +- configurations by $\mp \langle dp_T \rangle \times A_{LL}^{dp_T}$.



- Assign as a systematic uncertainty to measured jet A_{LL} as a function of jet p_T
- Underlying event systematic uncertainty is at the level of 10^{-4}
- Comparable in size with the relative luminosity uncertainty

STAR Jet Simulations



- Systematics study: PYTHIA + GEANT + Zero-bias events as **embedding** sample
- Data-driven modified PYTHIA Perugia Tune
- Jet reconstruction at three levels:
from the embedding sample **detector** jets and from PYTHIA **particle** and **parton** jets

Monte Carlo Tune Study

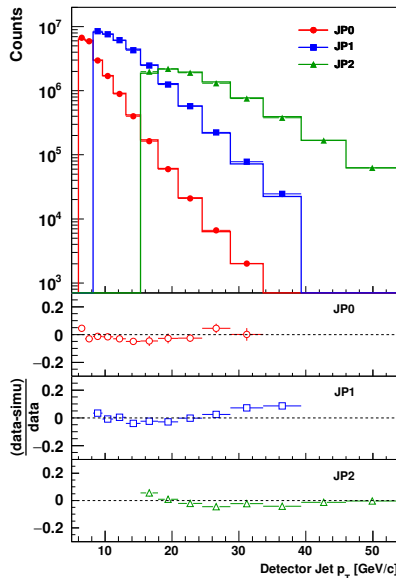
Markers: data and lines: simulation

- Tuning based on matching between PYTHIA simulation and previous STAR charged π^\pm spectrum measurements STAR, PLB 637, 161 and STAR, PRL 108, 072302
- Default Perugia 2012 tune except a smaller $p_{T,0}$ scale parameter, $P_{90} = 0.213$ default 0.24

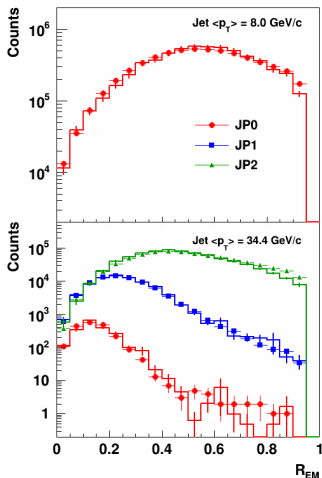
$$\sigma \sim \frac{1}{(p_T^2 + p_{T,0}^2)^2}$$

$$p_{T,0} = p_{T,ref} \times \left(\frac{\sqrt{s}}{\sqrt{s_{ref}}} \right)^{P_{90}}$$

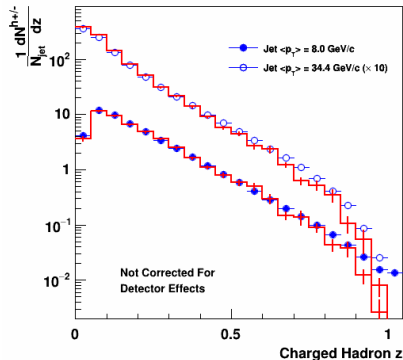
- Reduce multiple parton interaction contribution
- Jet spectrum comparison for three jet patch triggers, JP0, JP1 and JP2



Jet Neutral Energy Fraction and Charged Hadron z Comparison



- Jet $R_{EM} = \frac{\sum_{tower} E_T}{\sum_{tower} E_T + \sum_{track} p_T}$ distributions for two jet p_T bins



- Distributions of the longitudinal momentum fraction, z , of charged hadrons within jet for two jet p_T bins

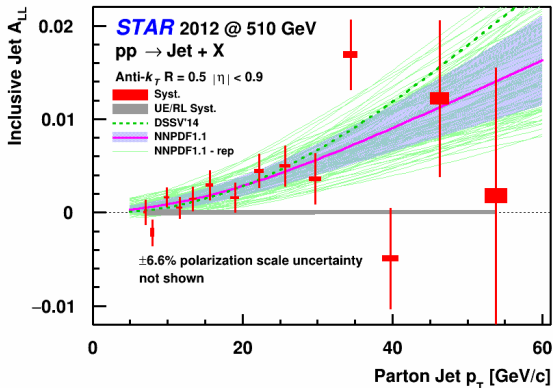
Simulation reproduces jet and its substructure variables well.

Systematic Uncertainty and Corrections

- Jet p_T and dijet M_{inv} are corrected back to parton level to facilitate the comparison between our results and recent NLO theoretical calculations
 - Through matching detector jets to parton jets in the embedding sample,
 $\Delta R = \sqrt{\Delta\eta^2 + \Delta\phi^2} < 0.5$
- Trigger bias and reconstruction correction and systematic uncertainty
 - Taking the difference of predicted jet A_{LL} between the unbiased parton level A_{LL} and the biased detector level A_{LL} , $\delta A_{LL} = A_{LL,parton} - A_{LL,detector}$
↓
 - Calculating δA_{LL} from published 100 replicas from the NNPDFpol1.1
↓
 - The average of δA_{LL} taken as the correction on measured A_{LL}
↓
 - The RMS of δA_{LL} taken as the systematic uncertainty on A_{LL}

STAR 510 GeV Inclusive Jet A_{LL} Results

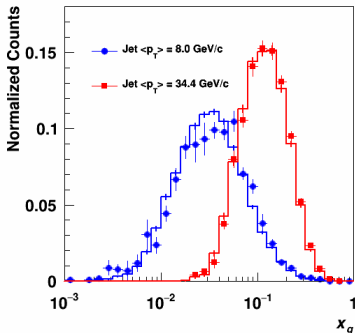
- Inclusive jet A_{LL} vs. parton jet p_T at $\sqrt{s} = 510$ GeV, STAR, Phys. Rev. D 100, 052005



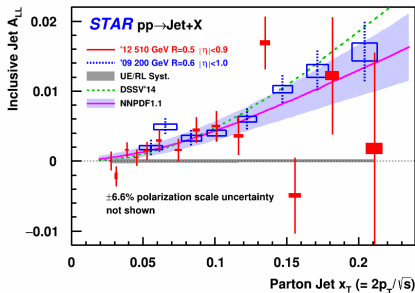
- Lowest measured jet p_T bin: $6.0 < p_T < 7.0$ GeV/c corresponding to parton jet $p_T = 7.02 \pm 0.26$ GeV/c
- Much reduced systematic uncertainty than the previous measurements at $\sqrt{s} = 200$ GeV
- Agree well with recent polarized PDF predictions, which is consistent with 200 GeV findings and implies **positive ΔG**

STAR 510 GeV Inclusive Jet A_{LL} Measurements

- Sample x_g distributions for two jet p_T bins, with $\langle p_T \rangle = 8.0$ and 34.4 GeV/c

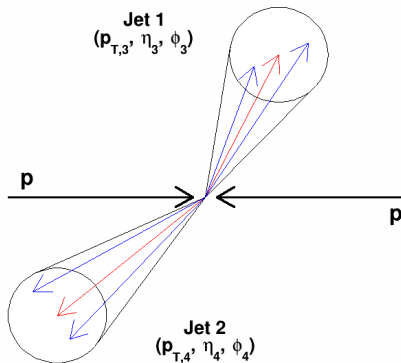


- Inclusive jet A_{LL} vs. jet $x_T = \frac{2p_T}{\sqrt{s}}$ together with 2009 200 GeV results



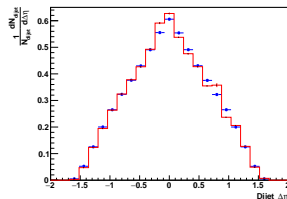
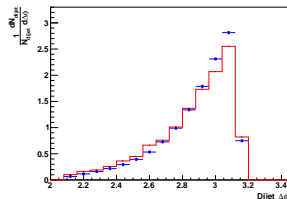
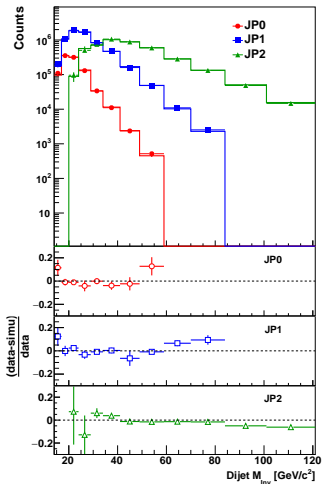
- At $\sqrt{s} = 510$ GeV, be able to measure jet A_{LL} at $x_T < 0.05$
- In the overlapping $x_T = \frac{2p_T}{\sqrt{s}}$ region, both results agree well
- Allow to access x_g as low as **0.015**

Dijet Event at $\sqrt{s} = 510$ GeV



- Opening angle $\Delta\phi = \phi_3 - \phi_4 > \frac{2\pi}{3}$, remove hard gluon emissions
- $|\Delta\eta| = |\eta_3 - \eta_4| < 1.6$, limit detector acceptance
- $\frac{p_T^{leading}}{p_T^{away}} < (6 - 0.08p_T^{max})$, where p_T^{max} is the highest track p_T in either jet, remove fake jets that are composed nearly of a single, poorly reconstructed TPC track
- $p_{3,T} > 6$ GeV/c, $p_{4,T} > 8$ GeV/c, theoretical consideration

Data Simulation Comparison for Dijet Quantities



- Dijet invariant mass spectra for jet patch triggers, JP0, JP1 and JP2
- Dijet $\Delta\phi$ and $\Delta\eta$ for jet patch triggers, JP0, JP1 and JP2 combined

Simulation reproduces dijet variables well too.

- Dijet A_{LL} vs. invariant mass for four η topologies

$$x_1 = \frac{1}{\sqrt{s}}(p_{T,3}e^{\eta_3} + p_{T,4}e^{\eta_4})$$

$$x_2 = \frac{1}{\sqrt{s}}(p_{T,3}e^{-\eta_3} + p_{T,4}e^{-\eta_4})$$

$$|\cos\theta^*| = \tanh\frac{|\eta_3 - \eta_4|}{2}$$

A/Forward-Forward:

$$0.3 < |\eta_{3,4}| < 0.9, \eta_3 \cdot \eta_4 > 0$$

B/Forward-Central:

$$|\eta_{3,4}| < 0.3, 0.3 < |\eta_{3,4}| < 0.9$$

C/Central-Central:

$$|\eta_{3,4}| < 0.3$$

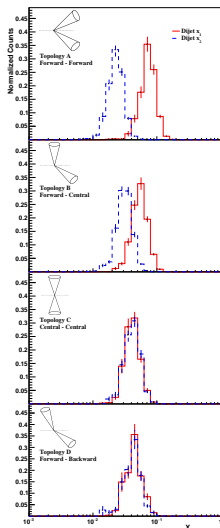
D/Forward-Backward:

$$0.3 < |\eta_{3,4}| < 0.9, \eta_3 \cdot \eta_4 < 0$$

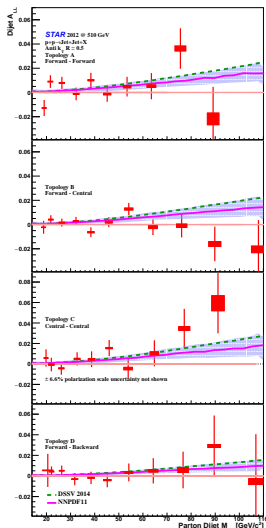


- Topology binning narrows the sampled x_g and the $\cos\theta^*$ ranges

STAR 510 GeV Dijet A_{LL} Results



- x_1 and x_2 distributions sampled by dijet invariant mass bin,
 $17 < M_{inv} < 20 \text{ GeV}/c^2$



- Dijet A_{LL} for η topologies vs. dijet M_{inv}

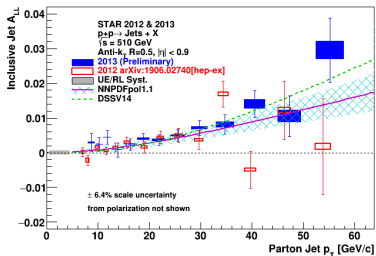
- STAR, Phys. Rev. D 100, 052005
- Dijet A_{LL} agree well with the NLO PDF model predictions
- Different sampled x_1 and x_2 distributions by four η topology bins
- Sampled x_g distributions much narrower than those from inclusive jets

Other inclusive jet and dijet A_{LL} measurements and STAR forward upgrade

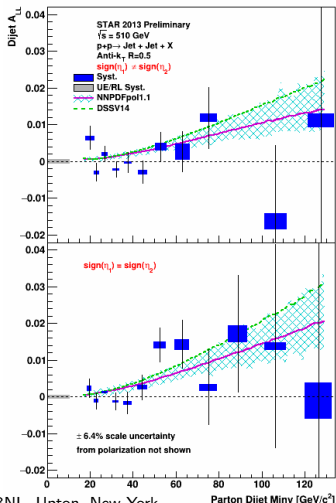


Inclusive and Dijet A_{LL} from STAR 2013 510 GeV Data

- STAR 2013 longitudinally polarized pp runs: $L = 300\text{pb}^{-1}$, and $P_{B,Y} \sim 51\%$, 52%
- Preliminary inclusive jet (left) and dijet (right) A_{LL} from STAR 2013 510 GeV data, Quintero, arXiv:1809.00923 [nucl-ex]

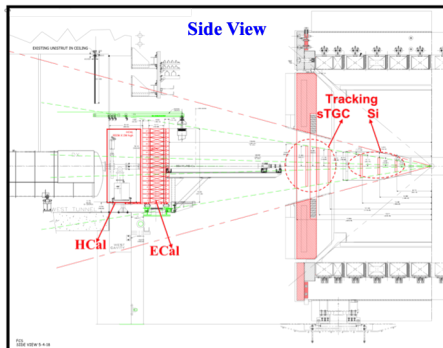


- Same procedure being applied as in 2012 $\sqrt{s} = 510 \text{ GeV}$ data
- The 2012 and 2013 results agree well
- Two η topologies for dijet A_{LL} , as in 2009 200 GeV scheme
- The study of the final systematic uncertainty is underway



STAR Forward Upgrade

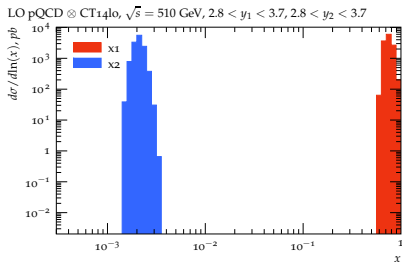
- STAR forward upgrade has been fully funded and approved in time for polarized 510 GeV run in 2022
- Forward Calorimeter System (FCS), an EMCal and a HCal
- Forwarding Tracking System (FTS), silicon detectors (Si) and small thin gap chamber (sTGC)
- pp , pA and AA in parallel with sPHENIX
- Lay the groundwork for the realization of the future Electron Ion Collider (EIC)



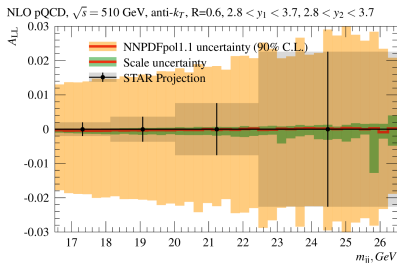
<https://drupal.star.bnl.gov/STAR/starnotes/public/sn0648>

Dijet Measurements with STAR Forward Upgrade

- Dijet measurements with one or both jets in the forward region ($2.8 < \eta < 3.7$) will be one of the highlighted measurements



Sampled x_1 and x_2 distributions
when both jets in the forward region

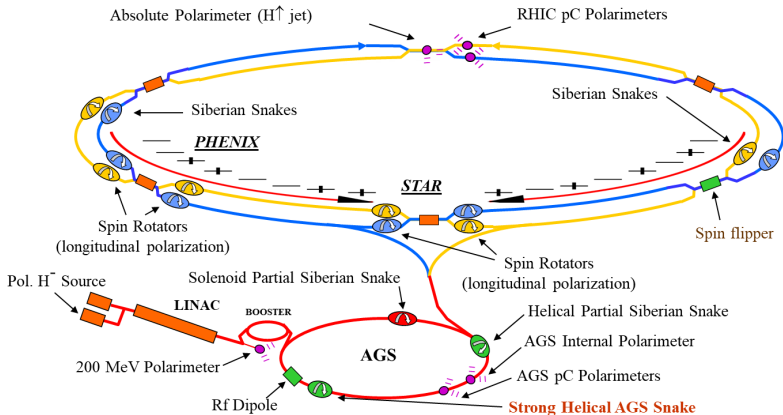


Predicted precision on dijet A_{LL} vs.
invariant mass, m_{jj} with
NNPDFpol1.1 model predictions

- At $\sqrt{s} = 510$ GeV, with both jets in the FCS, it will provide gluon polarization at $x_g \sim 10^{-3}$
- Significantly high precision on dijet A_{LL} comparing to the current model prediction

- STAR inclusive jet and dijet double-spin asymmetry measurements are unique to explore gluon polarization in the proton
 - ① Inclusive jets constrain the magnitude of the gluon polarization
 - ② Dijets constrain the shape of $\Delta g(x)$
- The 200 GeV results provided the first evidence of the positive gluon polarization
- **The first measured 510 GeV results will extend gluon polarization down to $x \sim 0.015$, STAR, Phys. Rev. D 100, 052005**
- Inclusive jet and dijet A_{LL} are being studied with the larger 2013 pp data at $\sqrt{s} = 510$ GeV
- The forward upgrade will provide new opportunities to probe low $x \sim 10^{-3}$ gluon polarization where the current polarized PDF studies show large uncertainties

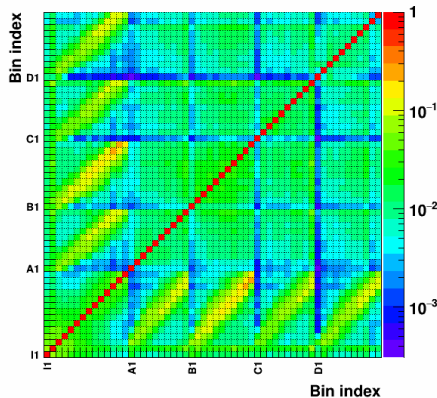
RHIC Facilities



- 120 RF bunches for each ring with 100 billion protons per bunch.
- Polarization orientation varies from bunch to bunch.
- Spin rotators provide choice of polarization orientation (longitudinal or transverse).
- Beam polarizations are around 55 to 65%

Correlations among Inclusive Jet p_T Bins and Dijet M_{inv} Bins

- Correlations arise due to:
 - Statistically in the same event, one or both of the two jets in the dijet event end up an inclusive jet
 - Systematically the way the systematic uncertainty is estimated, normally fully correlated across bins
- 14 inclusive jet p_T bins + 10 top-A dijet M_{inv} + 11 top-B dijet M_{inv} + 10 top-C dijet M_{inv} + 11 top-D dijet M_{inv} = 56 bins
- Correlations from relative luminosity uncertainty and beam polarization uncertainty not included



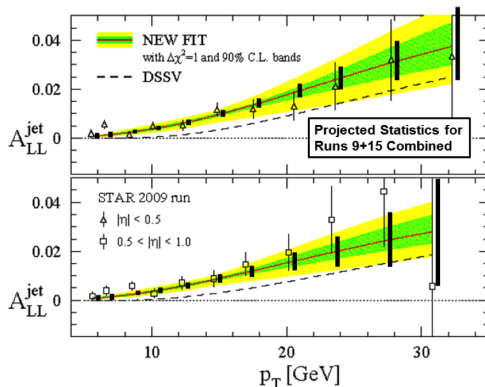
Longitudinally polarized pp Dataset at STAR

- Selected longitudinally polarized pp datasets at $\sqrt{s} = 200$ and 510 GeV:

Year	\sqrt{s} (GeV)	Recorded Luminosity (pb^{-1})	B/Y polarization $\langle P \rangle$
2009	200	25	55
2012	510	82	50/53
2013	510	300	51/52
2015	200	52	53/57

- 2009 and 2012 data are in publication
- 2013 and 2015 data are under analysis

Increased Precision for 200 GeV Inclusive Jet A_{LL}^{jet}



- 2015 longitudinally polarized pp run: luminosity 52 pb^{-1} and $P_{B,Y} \sim 53, 57 \%$
- The combined results from 2015 200 GeV data and the previously published 2009 data will reduce the statistical uncertainty by a factor of 1.6

STAR Charged π^\pm Spectrum

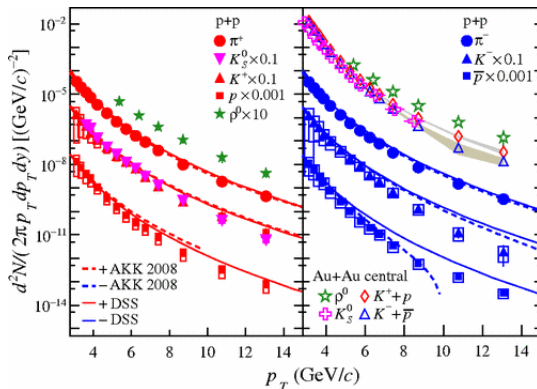


Figure: STAR charged π^\pm yields. STAR, PRL 108, 072302, 2012